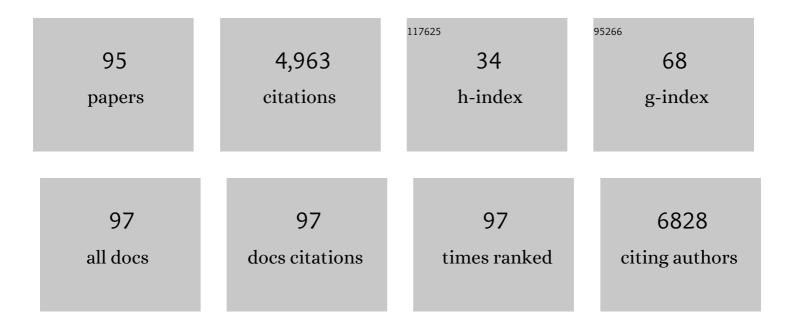
List of Publications by Year in descending order

Source: https://exaly.com/author-pdf/669250/publications.pdf Version: 2024-02-01



DONC PIP KIM

#	Article	IF	CITATIONS
1	Branched TiO <sub>2</sub> Nanorods for Photoelectrochemical Hydrogen Production. Nano Letters, 2011, 11, 4978-4984.	9.1	843
2	Single and Tandem Axial <i>p-i-n</i> Nanowire Photovoltaic Devices. Nano Letters, 2008, 8, 3456-3460.	9.1	401
3	Codoping titanium dioxide nanowires with tungsten and carbon for enhanced photoelectrochemical performance. Nature Communications, 2013, 4, 1723.	12.8	249
4	BiVO <sub>4</sub> /WO <sub>3</sub> /SnO <sub>2</sub> Double-Heterojunction Photoanode with Enhanced Charge Separation and Visible-Transparency for Bias-Free Solar Water-Splitting with a Perovskite Solar Cell. ACS Applied Materials & Interfaces, 2017, 9, 1479-1487.	8.0	158
5	SiO2 microparticles with carbon nanotube-derived mesopores as an efficient support for enzyme immobilization. Chemical Engineering Journal, 2019, 359, 1252-1264.	12.7	154
6	Hybrid Si Microwire and Planar Solar Cells: Passivation and Characterization. Nano Letters, 2011, 11, 2704-2708.	9.1	151
7	Synthesis of cross-linked protein-metal hybrid nanoflowers and its application in repeated batch decolorization of synthetic dyes. Journal of Hazardous Materials, 2018, 347, 442-450.	12.4	145
8	Enhancement of photo-thermal conversion using gold nanofluids with different particle sizes. Energy Conversion and Management, 2016, 112, 21-30.	9.2	128
9	Fabricating nanowire devices on diverse substrates by simple transfer-printing methods. Proceedings of the United States of America, 2010, 107, 9950-9955.	7.1	123
10	Frosting characteristics on hydrophobic and superhydrophobic surfaces: A review. Energy Conversion and Management, 2017, 138, 1-11.	9.2	120
11	Fabrication of Flexible and Vertical Silicon Nanowire Electronics. Nano Letters, 2012, 12, 3339-3343.	9.1	107
12	Fabrication of Nanowire Electronics on Nonconventional Substrates by Water-Assisted Transfer Printing Method. Nano Letters, 2011, 11, 3435-3439.	9.1	98
13	Transfer Printing Methods for Flexible Thin Film Solar Cells: Basic Concepts and Working Principles. ACS Nano, 2014, 8, 8746-8756.	14.6	89
14	Functional cooperation of the glycine synthase-reductase and Wood–Ljungdahl pathways for autotrophic growth of <i>Clostridium drakei</i> . Proceedings of the National Academy of Sciences of the United States of America, 2020, 117, 7516-7523.	7.1	88
15	Insights into Cell-Free Conversion of CO <sub>2</sub> to Chemicals by a Multienzyme Cascade Reaction. ACS Catalysis, 2018, 8, 11085-11093.	11.2	87
16	Direct growth of cerium oxide nanorods on diverse substrates for superhydrophobicity and corrosion resistance. Applied Surface Science, 2015, 340, 96-101.	6.1	74
17	Vertical Transfer of Uniform Silicon Nanowire Arrays via Crack Formation. Nano Letters, 2011, 11, 1300-1305.	9.1	73
18	Probing Flow Velocity with Silicon Nanowire Sensors. Nano Letters, 2009, 9, 1984-1988.	9.1	72

#	Article	IF	CITATIONS
19	Peel-and-Stick: Fabricating Thin Film Solar Cell on Universal Substrates. Scientific Reports, 2012, 2, 1000.	3.3	66
20	Thermal conductivity in porous silicon nanowire arrays. Nanoscale Research Letters, 2012, 7, 554.	5.7	64
21	Numerical Characterization and Optimization of the Microfluidics for Nanowire Biosensors. Nano Letters, 2008, 8, 3233-3237.	9.1	60
22	Hierarchical Macroporous Particles for Efficient Whole-Cell Immobilization: Application in Bioconversion of Greenhouse Gases to Methanol. ACS Applied Materials & Interfaces, 2019, 11, 18968-18977.	8.0	57
23	Visibly Clear Radiative Cooling Metamaterials for Enhanced Thermal Management in Solar Cells and Windows. Advanced Functional Materials, 2022, 32, 2105882.	14.9	51
24	Bioresorbable, Miniaturized Porous Silicon Needles on a Flexible Water-Soluble Backing for Unobtrusive, Sustained Delivery of Chemotherapy. ACS Nano, 2020, 14, 7227-7236.	14.6	50
25	Acetogenic bacteria utilize light-driven electrons as an energy source for autotrophic growth. Proceedings of the National Academy of Sciences of the United States of America, 2021, 118, .	7.1	47
26	A novel louvered fin design to enhance thermal and drainage performances during periodic frosting/defrosting conditions. Energy Conversion and Management, 2016, 110, 494-500.	9.2	45
27	Determination of the Genome and Primary Transcriptome of Syngas Fermenting Eubacterium limosum ATCCÂ8486. Scientific Reports, 2017, 7, 13694.	3.3	44
28	Adaptive Laboratory Evolution of Eubacterium limosum ATCC 8486 on Carbon Monoxide. Frontiers in Microbiology, 2020, 11, 402.	3.5	44
29	Methane oxidation over catalytic copper oxides nanowires. Proceedings of the Combustion Institute, 2011, 33, 3169-3175.	3.9	42
30	Thermal performance of microchannel heat exchangers according to the design parameters under the frosting conditions. International Journal of Heat and Mass Transfer, 2014, 71, 626-632.	4.8	42
31	Orientation-Controlled Alignment of Axially Modulated pn Silicon Nanowires. Nano Letters, 2010, 10, 5116-5122.	9.1	39
32	Flexible elastomer patch with vertical silicon nanoneedles for intracellular and intratissue nanoinjection of biomolecules. Science Advances, 2018, 4, eaau6972.	10.3	39
33	Genome Engineering of <i>Eubacterium limosum</i> Using Expanded Genetic Tools and the CRISPR-Cas9 System. ACS Synthetic Biology, 2019, 8, 2059-2068.	3.8	38
34	Modeling of frost layer growth considering frost porosity. International Journal of Heat and Mass Transfer, 2018, 126, 980-988.	4.8	37
35	Experimental investigation of frost retardation for superhydrophobic surface using a luminance meter. International Journal of Heat and Mass Transfer, 2015, 87, 491-496.	4.8	36
36	Genome-scale analysis of syngas fermenting acetogenic bacteria reveals the translational regulation for its autotrophic growth. BMC Genomics, 2018, 19, 837.	2.8	36

#	Article	IF	CITATIONS
37	Frosting behaviors and thermal performance of louvered fins with unequal louver pitch. International Journal of Heat and Mass Transfer, 2016, 95, 499-505.	4.8	35
38	Local frosting behavior of a plated-fin and tube heat exchanger according to the refrigerant flow direction and surface treatment. International Journal of Heat and Mass Transfer, 2013, 64, 751-758.	4.8	34
39	Optimum hub height of a wind turbine for maximizing annual net profit. Energy Conversion and Management, 2015, 100, 90-96.	9.2	34
40	Correlation of cross-cut cylindrical heat sink to improve the orientation effect of LED light bulbs. International Journal of Heat and Mass Transfer, 2015, 84, 821-826.	4.8	34
41	Fabrication of three-dimensional metal-graphene network phase change composite for high thermal conductivity and suppressed subcooling phenomena. Energy Conversion and Management, 2017, 149, 608-615.	9.2	34
42	Stochastic approach to the anti-freezing behaviors of superhydrophobic surfaces. International Journal of Heat and Mass Transfer, 2017, 106, 841-846.	4.8	34
43	Electroassisted Transfer of Vertical Silicon Wire Arrays Using a Sacrificial Porous Silicon Layer. Nano Letters, 2013, 13, 4362-4368.	9.1	33
44	Microscopic observation of frost behaviors at the early stage of frost formation on hydrophobic surfaces. International Journal of Heat and Mass Transfer, 2016, 97, 861-867.	4.8	33
45	Frost layer growth behavior under cryogenic conditions. Applied Thermal Engineering, 2019, 163, 114333.	6.0	33
46	Biodegradable silicon nanoneedles for ocular drug delivery. Science Advances, 2022, 8, eabn1772.	10.3	31
47	Direct Growth of Nanowire Logic Gates and Photovoltaic Devices. Nano Letters, 2010, 10, 1050-1054.	9.1	29
48	Frost growth mechanism and its behavior under ultra-low temperature conditions. International Journal of Heat and Mass Transfer, 2021, 169, 120941.	4.8	28
49	Frosting and defrosting behavior of slippery surfaces and utilization of mechanical vibration to enhance defrosting performance. International Journal of Heat and Mass Transfer, 2018, 125, 858-865.	4.8	27
50	Frost modeling under cryogenic conditions. International Journal of Heat and Mass Transfer, 2020, 161, 120250.	4.8	25
51	Shrinking and Growing: Grain Boundary Density Reduction for Efficient Polysilicon Thin-Film Solar Cells. Nano Letters, 2012, 12, 6485-6491.	9.1	24
52	Facile Fabrication of Superomniphobic Polymer Hierarchical Structures for Directional Droplet Movement. ACS Applied Materials & Interfaces, 2017, 9, 9213-9220.	8.0	24
53	Fabrication of micro-patterned aluminum surfaces for low ice adhesion strength. Applied Surface Science, 2018, 440, 643-650.	6.1	24
54	Rapid custom prototyping of soft poroelastic biosensor for simultaneous epicardial recording and imaging. Nature Communications, 2021, 12, 3710.	12.8	24

#	Article	IF	CITATIONS
55	Quantitative analysis of anti-freezing characteristics of superhydrophobic surfaces according to initial ice nuclei formation time and freezing propagation velocity. International Journal of Heat and Mass Transfer, 2018, 126, 109-117.	4.8	21
56	Enhanced thermal performance of phase change material-integrated fin-type heat sinks for high power electronics cooling. International Journal of Heat and Mass Transfer, 2022, 184, 122257.	4.8	21
57	Defrosting behavior and performance on vertical plate for surfaces of varying wettability. International Journal of Heat and Mass Transfer, 2018, 120, 481-489.	4.8	20
58	Recent progress on developing anti-frosting and anti-fouling functional surfaces for air source heat pumps. Energy and Buildings, 2020, 223, 110139.	6.7	20
59	Local frost behaviors of a scaled-up louvered fin heat exchanger. International Journal of Heat and Mass Transfer, 2015, 89, 1127-1134.	4.8	19
60	Thermal performance improvement based on the partial heating position of a heat sink. International Journal of Heat and Mass Transfer, 2018, 124, 752-760.	4.8	19
61	Numerical modeling and experimental validation of a phase change material-based compact cascade cooling system for enhanced thermal management. Applied Thermal Engineering, 2020, 164, 114470.	6.0	19
62	Granular temperature and rotational characteristic analysis of a gas–solid bubbling fluidized bed under different gravities using discrete hard sphere model. Powder Technology, 2015, 271, 35-48.	4.2	18
63	Numerical characterization of micro-cell UO2Mo pellet for enhanced thermal performance. Journal of Nuclear Materials, 2016, 477, 88-94.	2.7	18
64	Threeâ€Dimensionally Programmed Slippery Wrinkles with High Stretchability for Tunable Functionality of Icephobicity and Effective Water Harvesting. Advanced Materials Interfaces, 2018, 5, 1800980.	3.7	18
65	Enhanced water collection of bio-inspired functional surfaces in high-speed flow for high performance demister. Desalination, 2020, 479, 114314.	8.2	14
66	Frost behavior of a louvered fin heat exchanger with vortex-generating fins. International Journal of Heat and Mass Transfer, 2017, 114, 590-596.	4.8	13
67	Minimizing thermal interference effects of multiple heat sources for effective cooling of power conversion electronics. Energy Conversion and Management, 2018, 174, 218-226.	9.2	13
68	Enhanced thermal performance of lithium nitrate phase change material by porous copper oxide nanowires integrated on folded meshes for high temperature heat storage. Chemical Engineering Journal, 2020, 391, 123613.	12.7	13
69	Fabrication of three-dimensional porous carbon scaffolds with tunable pore sizes for effective cell confinement. Carbon, 2018, 130, 814-821.	10.3	12
70	Frost formation from general-low to ultra-low temperatures: A review. International Journal of Heat and Mass Transfer, 2022, 195, 123164.	4.8	12
71	Cooling performance and space efficiency improvement based on heat sink arrangement for power conversion electronics. Applied Thermal Engineering, 2020, 164, 114458.	6.0	11
72	Investigating the role of metals loaded on nitrogen-doped carbon-nanotube electrodes in electrodes in electroenzymatic alcohol dehydrogenation. Applied Catalysis B: Environmental, 2022, 307, 121195.	20.2	11

#	Article	IF	CITATIONS
73	Genome-scale analysis of <i>Acetobacterium bakii</i> reveals the cold adaptation of psychrotolerant acetogens by post-transcriptional regulation. Rna, 2018, 24, 1839-1855.	3.5	10
74	Controlled Integration of Interconnected Pores under Polymeric Surfaces for Low Adhesion and Antiscaling Performance. ACS Applied Materials & amp; Interfaces, 2021, 13, 13684-13692.	8.0	10
75	Optical investigation of cryogenic frost formation under forced convection. Applied Thermal Engineering, 2022, 202, 117887.	6.0	10
76	Numerical and experimental investigation on thermal expansion of UO2-5 vol% Mo microcell pellet for qualitative comparison to UO2 pellet. Journal of Nuclear Materials, 2019, 518, 342-349.	2.7	9
77	Modeling of frost growth and fog generation at ultra-low temperatures. International Journal of Heat and Mass Transfer, 2021, 166, 120741.	4.8	9
78	Frost layer growth behavior on ultra-low temperature surface with a superhydrophobic coating. International Communications in Heat and Mass Transfer, 2021, 128, 105641.	5.6	9
79	Rotation characteristic and granular temperature analysis in a bubbling fluidized bed of binary particles. Particuology, 2015, 18, 76-88.	3.6	8
80	Sensor-Instrumented Scaffold Integrated with Microporous Spongelike Ultrabuoy for Long-Term 3D Mapping of Cellular Behaviors and Functions. ACS Nano, 2019, 13, 7898-7904.	14.6	8
81	Genome-Scale Analysis of Acetobacterium woodii Identifies Translational Regulation of Acetogenesis. MSystems, 2021, 6, e0069621.	3.8	8
82	Three-Dimensional Hetero-Integration of Faceted GaN on Si Pillars for Efficient Light Energy Conversion Devices. ACS Nano, 2017, 11, 6853-6859.	14.6	7
83	Power optimization for defrosting heaters in household refrigerators to reduce energy conversion and Management, 2021, 237, 114127.	9.2	7
84	Direct growth of hierarchical nanoneedle arrays with branched nanotubes from titanium foil with excellent anti-corrosion and superhydrophilicity. Chemical Engineering Journal, 2019, 372, 616-623.	12.7	6
85	Layer-by-layer assembled phase change composite with paraffin for heat spreader with enhanced cooling capacity. Energy Conversion and Management, 2020, 204, 112287.	9.2	6
86	Evaluation of thermomechanical behaviors of UO2-5 vol% Mo nuclear fuel pellets with sandwiched configuration. Journal of Nuclear Materials, 2020, 539, 152295.	2.7	6
87	Water-repellent Hybrid Nanowire and Micro-scale Denticle Structures on Flexible Substrates of Effective Air Retention. Scientific Reports, 2018, 8, 16631.	3.3	5
88	3D Printed Bioresponsive Devices with Selective Permeability Inspired by Eggshell Membrane for Effective Biochemical Conversion. ACS Applied Materials & Interfaces, 2020, 12, 30112-30119.	8.0	5
89	Replicable Quasi-Three-Dimensional Plasmonic Nanoantennas for Infrared Bandpass Filtering. ACS Applied Materials & Interfaces, 2021, 13, 24024-24031.	8.0	4
90	Bactericidal Lubricating Synthetic Materials for Three-Dimensional Additive Assembly with Controlled Mechanical Properties. ACS Applied Materials & Interfaces, 2020, 12, 26464-26475.	8.0	3

# Article	IF	CITATIONS
91 High quality GaN tetrapodal structures hetero-integrated on 3D Si surface 2021, 565, 150584.	es. Applied Surface Science, 6.1	1
92 Compact Model of Slug Flow in Microchannels. , 2007, , .		1
93 3-D Numerical Simulation of Contact Angle Hysteresis for Slug Flow in M	icrochannel. , 2007, , 955.	Ο
94 Fabrication of nanowire electronics on nonconventional substrates by w printing method. Proceedings of SPIE, 2015, , .	ater-assisted transfer 0.8	0
Slippery Materials: Threeâ€Dimensionally Programmed Slippery Wrinkles 75 Tunable Functionality of Icephobicity and Effective Water Harvesting (Ac Advanced Materials Interfaces, 2018, 5, 1870104.	with High Stretchability for v. Mater. Interfaces 21/2018). 3.7	Ο